ORIGINAL ARTICLE

European Journal of Applied Physics
www.ej-physics.org

Radiation Induced Defects and Thermoluminescence Characteristics in Eu, Dy and Eu/Dy Doped-Quartz Sol-Gel by 2 Gy Beta and 2 MeV $^4He^+$ Irradiations

F. Khamis and D.-E. Arafah

ABSTRACT

Thermoluminescence (TL) of pure and Eu^{3+} and Dy^{3+} doped synthesis quartz was synthesized and their ion beam and thermoluminescence properties were investigated. The as prepared, doped and co-doped quartz and the effects of imparting 2 Gy beta dose and 2MeV $^4He^+$ ion beam irradiation is investigated. The basic model proposed and can explain our observations is that, the dominant signals from the as prepared material arise from the incorporation of the transitions within the RE dopants enhanced by the intensity from the intrinsic or host defect sites within the synthesis quartz network. The complex shape TL glow curves indicate that irradiation causes major distortions to the lattice with the incorporation of extrinsic impurities and RE doping processes, induce perturbations and alter the energy levels pattern of the free ions and assigned transitions probabilities in a manner that that depends on the dopants, their concentrations and the host material. The larger Eu ions stabilize the emission more than that of the Dy ions. The TL peak temperatures are commonly correlated via charge transfer processes and scale with the ions size, in such a manner that the close proximity (or shallow traps) allows lower temperature electron release, whereas the more distant variants (deep traps) are less distorted, but are still able to couple to the higher energy orbitals of the Eu ions.

Keywords: Defects; Ion beam, Rutherford backscattering; Thermoluminescence.

Published Online: October 13,2020

ISSN: 2684-4451

DOI:10.24018/ejphysics.2020.2.5.21

F. Khamis*
Department of Physics, University of Tripoli, Libya.
(e-mail: f.khamis@uot.edu.ly)

D.-E. Arafah
Department of Physics, The University of Jordan, Jordan.
(e-mail: darafah@ju.edu.jo)
On sabbatical at The higher Council for Science and Technology, HCST.
(e-mail: dia.arafah@hcst.gov.jo)

****Corresponding Author***

I. Introduction

Rare-earth elements have generally been recognized to have great demand in the commercial market owing to their unique magnetic, luminescent, catalytic, and electrochemical properties [1], [2]. The ever-growing demand for rare-earth enabled products and technologies has motivated researchers to improve the properties of the existing luminescent materials and to provide new novel materials of desired color, composition and optical properties [3]. Since glasses possess non-crystalline structure it is relatively easy to incorporate varying concentration of the dopant ions in the glass network. The glasses doped with rare-earth ions are of great importance due to their applications in lasers, amplifiers and lighting devices [4]. Owing to the excellent transparent property, silica glass is a key material of particular interest for many optical applications such as optical waveguide, optical components for photolithography. Silica-based glasses offer solubility for rare-earth ions of about 6×10^{20} cm^{-3}, are transparent in the visible to near-infrared region, and are easily compatible with Integrated Optics, IO- technology [2]. Applications in devices composing a network system use thin layers of amorphous SiO_2 (a-SiO_2) as a mask for selective ion implantation or insulation between metal and semiconductor layers [5], [6].

In other applications, devices with silica glass are exposed over a broad range of energies to different types of ion irradiations and thus controllably induce electrical, optical, structural, mechanical and chemical properties of materials for a broad range of research and applications, including advanced electro-optical devices and engineered nanostructures[7]-[9]. This, however, requires crucial understanding of the mechanism and processes of structural damage induced by the irradiation beam [10], [11]. Changes, including phase transformations and functional properties near surface regions of materials have been investigated in a series of conferences and proceedings on ion beam modification and analysis of materials (IBMM)-, see e.g. [12], [13]. Commonly, defects can be grouped according to their structure and size as point defects, dislocations (linear defects), and plane defects. The structural damage in crystalline materials include point defects, defect clusters, dislocations and amorphization zones [14]-[16]. The

European Journal of Applied Physics
www.ej-physics.org

literature about irradiation-induced phase transformation and structural modification, have been reported in many previous studies [17]-[20]. Radiation effects in silicate glasses and amorphous SiO_2designate that the energy dissipated in the glass matrix is through the atomic displacements produced by direct nuclear collisions and the ionization damage produced by interactions of the bombarding particles with the bonding electrons. A variety of ionizing conditions including swift proton, electron and gamma irradiation which focus on electronic excitations dominated irradiation processes, induce structural transformations from large ring structure to small three and four, member ring structures resulting with physical disorder to the glass network [21], [22]. Indeed, two types of structural damage have been identified in silica glasses; the intrinsic defects: the E'-centers, the peroxy radical and non-bridging oxygen hole center. The other type of structural damage is the physical disorder, induced by wide distribution of Si-O-Si bond angle. In addition to the defects present with un-paired electron, the limited knowledge of the neutral oxygen deficiency centers (ODCs) have received considerable attention, because they are also essential defects that affect the optical absorption in practical applications [23], [24]. However, ion beam is one of the alternative probes to detect absorption bands corresponding to non-relaxed oxygen vacancy, whereas luminescence measurements during ion irradiation allows one to measure the dynamic processes involved in damage creation and relaxation in the glass network [25], affected by impurities such as OH hydrogen [26], [27].

The interaction of ions with solids results in structural defects and damage to the material through the energy deposition to both the atomic nuclei and electrons in the solid. Energy is transferred to the electronic and atomic structures, and the corresponding response of materials, is divided into three principal energy regimes. At low incident ion energies, the transfer of energy to atomic nuclei (nuclear energy loss) dominates, leading to the displacement of atoms via elastic scattering collisions between atomic nuclei in ballistic collision cascades, while at high incident energies, the electronic energy loss dominates, leading to intense local ionization. At intermediate ion energies, however, nuclear and electronic energy losses are of similar magnitude, which can lead to additive effects on damage production [15]. The presence of impurities may cause the formation of defects and/or lead to the transformation of the existing defects to other types of defect. The distribution of intrinsic defects is usually combined and enhanced by the impurity(extrinsic) defects which activate materials to become novel to be recognized as interesting in the field of radiation dosimetry to explore new features and reveals potential applications, see e.g. [28]-[30].

To this end, the Thermoluminescence (TL) method has emerged as an important technique for understanding the dynamics of electron trapping centers. TL-glow curve analysis methods have been applied to study the kinetics of trapped electrons. Realizing that thermoluminescence (TL) is a defect related phenomenon, information about the presence of intrinsic and extrinsic impurity defects which markedly influence the TL-response and sensitivity of the material, can be pursued. This is possible and constitutes the first step in characterizing the materials under investigation, if the impurities, their concentration, stability, and depth distributions in the near surface regions of solids are determined. On the other hand, the analysis of ion induced luminescence in Rare Earth ions doped silica glass is complicated owing to the simultaneous measurement and dynamicity of the luminescent phenomenon. In the present study, we first examine the characteristics of luminescence activated by the addition of extrinsic impurities, namely Rare Earth- (RE-dysprosium (Dy) and europium (Eu) incorporated within the glass network and then investigate the structural properties. The evolution of radiation induced intrinsic and extrinsic defects on TL characteristics, caused by the energetic irradiation beam (i.e. $^4He^+$ ions)and changes caused to the glass network initially by the energy deposited to electronic excitations and near the end of the ions track by nuclear collisions is investigated.

II. Experimental

Samples were synthesized using sol-gel method following according to the procedure and technique previously described and reported [31]. Samples used in the measurements were shaped out in the form of circular discs (mass 15 mg), with dimensions: 5mm diameter and thickness about 1mm, under a pressure of 1.0-ton. All samples were then annealed at temperature about 1100 ^oC/2h in a platinum (Pt) crucible.

All measurements which include information about the defect structure and changes in the density and distribution of defect states are determined from the GL-curves followed using thermoluminescence (TL). Samples were measured directly after being subjected to pre-excitation source of a constant dose of 2Gy using ^{90}Sr-^{90}Y-β-particles emission source, supplied by VINTEN Model 623 automatic dosimeter irradiator of nominal activity 1mCi which, delivers the dose at a rate of 2.87μGy s^{-1}. Other samples were measured after excitations using 2 MeV $^4He^+$ beam supplied from the University of Jordan Van de Graff accelerator (JUVAC).

The system employed in TL detection, see, e.g. [32], [33]**,** was a Harshaw Model 3500 TLD reader. The TL-signal representing the intensity of light emitted as function of the simultaneously recorded time and temperature was obtained. All TL glow curves were read using a linear heating rate of 2 $^oCs^{-1}$, from room temperature up to 400 ^oC, with a preheat temperature set at 80 ^oC, to eliminate the more rapidly fading low temperature peaks in the TL glow curves and focus on the higher trapping states near the end of TL glow curve. Prior to readout, background signal due to black body radiation was recorded for all samples. The TL glow curves included inherent overlapping peak features, and therefore were deconvolved using total curve fitting technique assuming general order (GO) kinetic processes. The above procedure, however, ensures that peak centroids, intensity, and widths are all not disturbed by the analysis. More

European Journal of Applied Physics
www.ej-physics.org

detailed information about ion irradiation and TL measurements is found elsewhere [31], [33].

III. Results And Discussion

A. *Characterization of the samples*

The TL intensity in general depends on the particles sizes and on their impurities in the lattice of pure and synthesis quartz, Fig. 1 an illustrating diagram for the stages of preparation of silica glass by sol-gel method. Fig. 2 show the energy dispersive spectroscopy (EDS) analysis and the scanning electron microscopy (SEM) micrographs of the synthesis fraction extracted from the whole samples.

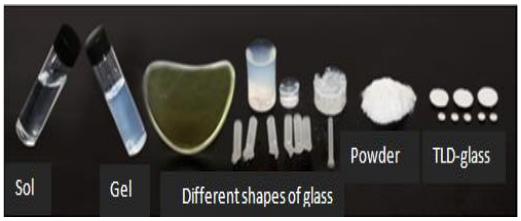

Fig. 1. Preparation stages of synthesis TLD-quartz by sol-gel technique, with different forms.

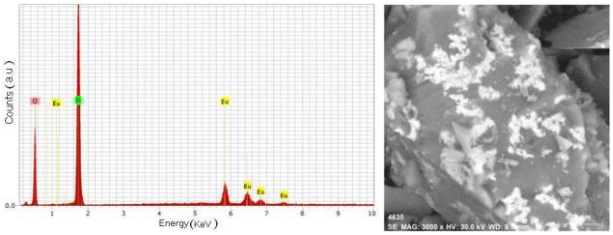

Fig.2.EDS analysis of doped synthesis quartz: Eu (0.002). In the inset, SEM micrographs.

B. *TL Glow-curve analysis of samples*

Typical TL glow curves of pure and doped synthesis quartz samples prepared by sol-gel comparing with natural quartz, All samples were annealed at 1100ºC are shown in Fig.3,measured at a constant heating rate $2Ks^{-1}$ after β irradiation of 2Gy. The quartz sample material's curve is characterized by the detection of relatively narrow and well resolved TL-peaks centered at 150ºC and 200ºC. The natural peak of quartz at 110ºC was partially detected but any trapping site with TL so close to room temperature will rapidly fade away due to its short lifetime and is irrelevant for dosimetric applications. The curves of samples prepared by sol-gel, are represented by two broad TL-peak structures of varying intensities that are detected within the temperature region 150 ºC and 300 ºC. And the resulting TL glow curves of samples of doped with Eu^{+3} and Dy^{+3}, respectively were found to exhibit the highest intensity for TL peaks. It is interesting to note that the dopant not only resulted in the detection of the new and high temperature TL-peaks, but also enhancement on the TL-response of the main dosimetric peak was noted. The shape of glow curve is different with doped and co-doped quartz, becomes same of the concentration for each Eu(0.2 mol%), Dy(0.002 mol%) and Eu/Dy, but results in a lower TL response and forms a sharp peak around 157ºC and the highest intensity for TL-peaks, whereas the intensity is about 5-times in comparison with doped Eu (0.2 mol%) samples.

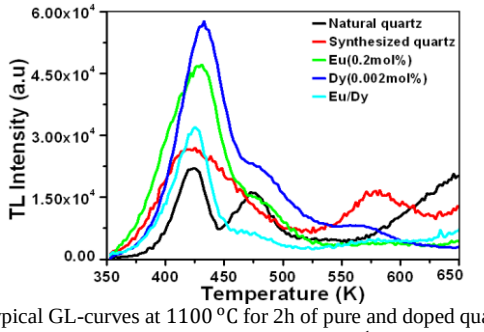

Fig. 3. Typical GL-curves at 1100 ºC for 2h of pure and doped quartz. GL-curves are measured at a constant heating rate 2 Ks^{-1} after imparting a total dose of 2 Gy.

They are emphasized that each of these doped samples were de-convoluted to the same number of peaks, in addition to a background signal. Such quantitative measures make the novel doped material excellent candidate to be used in dosimetry that requires high temperatures working environments. In any case, the kinetic parameters for each TL glow curve are listed in Table 1 for comparison and completeness.

The output of the calculation which represents the kinetic parameters, namely the trap depth (*E*), thermal or activation energy which is the energy needed to free the trapped electrons, the temperature at maximum (T_M), kinetic order (b), the frequency factor s, the pre-exponential factor and lifetime (τ) are listed in Table 1.

TABLE 1: Trapping Parameters Of Main Tl-Peaks Of Natural Quartz And Silica Glass Prepared By Sol-Gel Method As Determined Total Tl Glow Curve Deconvolution Technique

# of Traps	*Natural Quartz*				
	E(eV)	*T_m(K)*	*b*	*$s(s^{-1})$*	**τ*
P_1	1.24	423	1.10	9.57×10^{13}	12m
P_2	1.28	473	1.22	5.7×10^{12}	82y
P_3	1.29	505	1.34	8.75×10^{11}	808y
P_4	1.30	539	1.35	1.54×10^{11}	7.73×10^{3}y
P_5	1.31	613	1.46	4.53×10^{9}	3.47×10^{5}y
Synthesis Quartz by sol-gel method					
P_1	0.80	411	1.24	6.95×10^{8}	1.19d
P_2	0.86	439	1.36	8.31×10^{8}	12.32d
P_3	1.04	468	1.56	1.57×10^{10}	23.34m
P_4	1.05	505	1.72	2.81×10^{9}	19y
P_5	1.15	585	1.40	5.66×10^{8}	4.17×10^{3}y

C. *Irradiation of Rare Earth doped and co-doped synthesis quartz*

The effect of RE-doping: Eu or Dy and co-doping of the synthesis quartz with both Eu and Dy under different ionizing radiation on the TL properties of silica glass doped with 0.2 mol% of Eu, 0.002 mol% of Dy and co-doping with Eu/Dy, respectively, is shown in Fig.4. The TL glow curves of samples recorded between RT and 400ºC, illustrate the effect of 2 Gy β-dose irradiation compared to2 MeV $^4He^+$ irradiation beam to $1x10^{15}$ ions/cm^2. The TL glow curves of 2 Gy β-dose irradiation are generally distinguished by a prominent well defined narrow temperature peak centered near 150ºC and a varying intensity two broad peak structures detected in the higher temperature range 177-327 ºC.

European Journal of Applied Physics
www.ej-physics.org

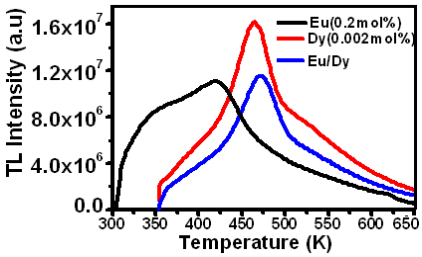

Fig. 4. Typical TL GL-curves showing the noted variations of TL-intensity and shapes between samples annealed 1100ºC/2h and representing single and double doped synthesis quartz. Measurements are recorded after 2MeV $^4He^+$ irradiation.

Comparing with the 2 MeV $^4He^+$ irradiation beam affected the synthesis quartz network structure in a more complex manner. In fact, the impurity activators that have been stimulated initially by electronic excitation and at the end of the ion track by the atomic displacement of the lattice. The disturbed region is extended to include the low and high temperature peak features indicating that the resulting TL glow curve is complex in structure, shape and analysis. The TL intensity of the prominent peak which is detected near 150ºC not only its intensity increased by about eighty folds, but also the satellite peaks near the low and high temperature regions are accompanied by an enormous increase of the whole TL glow curve. The inherent overlapping features observed add to its complexity through the energy deposition to nuclear and electronic excitations of the glass network [17].

The energy transfer processes that produce intrinsic defects within the glass network via electronic excitations (S_e) and atomic displacements (S_n) of 2 MeV He+ onto SiO_2. The corresponding total energy loss as well as the depth, and damage distributions induced in the glass network are shown. The curves of Fig.4 indicate opposite energy dependence with the radiation energy but an almost constant total energy loss within the energy range shown. In fact, the similar energy dependence gives evidence that all the three types of intrinsic defects are mainly produced by the nuclear energy loss or elastic collisions and the fact that the absolute value of Sn is smaller than that of Se also implies that Sn is more efficient in producing the damage and hence the intrinsic defect formation. Indeed, comparing the curves of Figs.3, suggests that the more efficient structural modifications of Sn in the formation of intrinsic defects than that of Se. Our results do not eliminate the role played by Se. Indeed, two types of intrinsic defect formation in synthesis quartz by electronic excitations. The first is the cleavage of a single Si-O bond forming E' center and NBOHC, simultaneously (Eq.1). An alternative mechanism is the displacement of a bridging oxygen atom forming an intestinal oxygen atom and two E' centers, where both E' centers can bond with each other forming =Si-Si=, (Eq.2)). Thus. the ration of concentration of E' center to NBOHC is generally about unity.

This implied that the damage caused by the energetic beam of 2MeV He^+ particles are far more efficient in causing damage by electronic processes which indeed exceeds that caused by nuclear processes.Examining such TL glow curves more closely, indicates that the resulted defect structure which is essentially a function of the concentration of activators is mobile. Indeed, Fig.4, gives evidence of shift of the peak maximum towards higher temperatures resulting from increasing the irradiation. One possible explanation is that radiative transition may be quenched at elevated temperatures as a result of an increased contribution of non-radiative transitions in the Eu^{3+}, Dy^{3+} or Eu/Dy: silica system or through energy transfer from excited RE^{3+} ions to other ions [34].

It is, however, suggested that special attention and focus is paid towards the progression of the prominent TL-peaks such that analyzing the deconvolved TL-peaks may provide information about the defects and mechanisms of charge carriers and recombination processes. It is suffice at this stage to provide a qualitative description and make an inter-comparison between the TL glow curves which include the prominent peaks characterizing their temperature at maximum positions, intensities and dose response. Such information is facilitated by calculating the parameters that characterize each TL-peak.For Such comparison to become meaningful, one additional condition must be imposed on the number of deconvolved TL-peaks inherent in the TL glow curves that must be preserved for possible association with NBOHC. Nonetheless, the recorded experimental Gl-curves have been de-convoluted into eight peaks, cf. Fig. 5. For all irradiated samples at 2Gy, the peaks are centered at 123 and 150 ºC with full width at half maximum (FWHM) 38 ºC, 37 ºC for Eu dopants; 157, 183 ºC with FWHM 42, 48ºCfor Dy dopants and finally for both dopants the peaks are centered at 150, 188ºC, with similar FWHM of 39 and 39 ºC, respectively. On the other hand, with samples irradiated by 2 MeV $^4He^+$ beam, a group of TL-peaks P_1toP_3; divalent Si (i.e. peak P_4), E'-center (i.e. peak P_5) with an extra band for P_6-P_8 corresponding to the $\equiv Si - Si \equiv$are found [23], [34], [35]. Furthermore, literature has reported that there are two major processes for intrinsic defects formation in silica glass by electron excitation. The first one is the cleavage of a single Si-O bond forming E'-center and NBOHC simultaneously, cf. Eq. (1).

$$\equiv Si - O - Si \equiv \rightarrow \equiv Si \cdot (E'center) + \cdot O - Si \equiv (NBOHC) \quad (1)$$

The second alternative possible mechanism is provided through the displacement of a bridging oxygen atom; thus forming an interstitial oxygen atom and two E' centers, such that the two E' centers can bond with each other forming $\equiv Si - Si \equiv$, cf. Eq. (2),namely:

$$\equiv Si - O - Si \equiv \rightarrow 2 \equiv Si \cdot (E'center) + \cdot O^0 \rightarrow \equiv Si - Si \equiv + O^0 \quad (2)$$

European Journal of Applied Physics
www.ej-physics.org

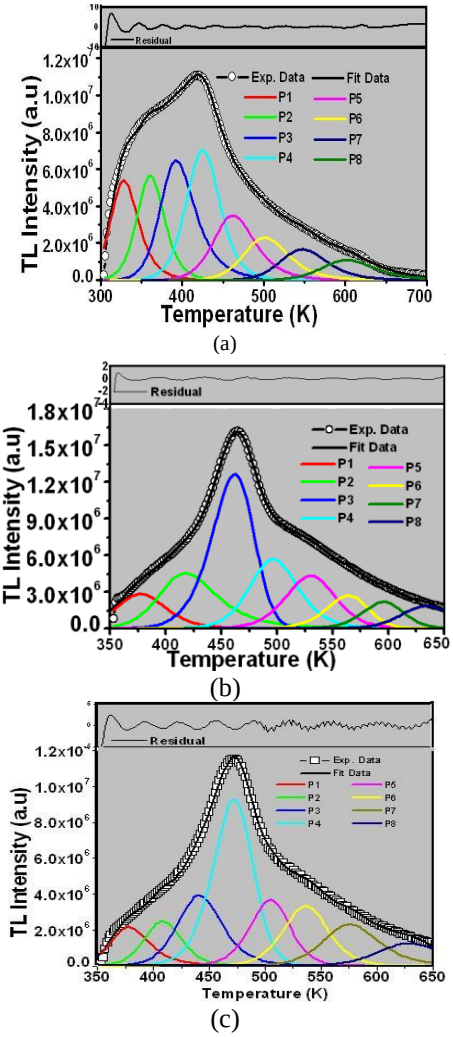

Fig. 5. Gl-curve decovolution analysis applied to SiO_2 doped with: (a) Eu(0.1mol%), (b) Dy(0.002mol%) and (c) co-doped: Eu(0.1mol%)/Dy(0.002mol%) after 2MeV $^4He^+$ irradiation.

By reference the de-convolution procedure carried out, TL characteristics related to trap parameters of different emission TL-peaks are thoroughly explored, which are mostly associated with electron-hole (i.e. exciton) pairs and oxygen defects sites related shallow and deep trap centers [28]. The trapping parameters are listed inTable 2. Comparison between the glow curves of doped and co-doped samples perturbation on the intensity is noted such that the intensity in some cases is doubled. The number of peaks, however, is preserved but there exist changes in their detected positions and perhaps their type. Literature indicates the formation of clusters and complex defect structure proceeding doping. The increase of intensity is solely due to incorporation of Eu, Dy, and Eu/Dy. Oxygen also has a role in enhancing the TL emission process by vacancy type defects[36].In general, oxygen impurities are known to be first physically adsorbed at the grain boundaries and on the glasses surface. One other hand, oxygen when present at the samples surface and at grain boundaries, it acts as luminescent centers [37]-[39]. In addition, the presence Eu, Dy and Eu/Dy impurities in the samples are trapped as shown at Eq (1) and Eq (2) defects. The defects capture free electrons generated after irradiation by highly energetic particles and act as electron traps.

The activation energy of the traps is observed to increase with the center of each trap shifted by some 30 K towards higher temperatures, as shown in Table 2. This seems to be a result of a highly populated trapping state and several recombination centers. The transition probabilities are substantially different from one peak to another due to variations in the trapping cross section. Notice the variation in b values where for all peaks Ps they exhibit a general order kinetic equation.

TABLE 2: TRAPPING PARAMETERS OF SIO2: EU, DY AND EU/DY AS OBTAINED FROM NUMERICAL FITTING TECHNIQUE

Defects	*# of Traps*	*RBS (2MeV)*				
		E(eV)	*T_m(K)*	*b*	*n_0*	*w(K)*
Eu (0.2mol%)	P1	0.697	331	1.74	1.362×10^7	41.12
	P2	0.909	361	1.91	1.274×10^5	39.97
	P3	0.977	393	2.5	1.907×10^5	50.50
	P4	1.024	426	1.86	1.923×10^5	48.42
	P5	1.040	462	2.14	1.208×10^5	60.30
	P6	1.139	502	2.13	8.532×10^4	64.63
	P7	1.315	547	2.16	6.482×10^4	67.41
	P8	1.389	602	2.1	4.828×10^4	77.45
Dy (0.002mol%)	P1	0.728	377	1.85	8.452×10^4	52.75
	P2	0.886	418	2.46	1.637×10^5	61.82
	P3	1.063	462	1.24	3.106×10^5	44.79
	P4	1.349	497	1.92	1.649×10^5	51.30
	P5	1.396	531	1.68	1.278×10^5	52.73
	P6	1.727	565	1.43	6.702×10^4	44.73
	P7	2.101	596	1.61	5.335×10^4	43.71
	P8	2.218	634	2.5	6.333×10^4	59.12
Eu/Dy	P1	1.122	378	2.44	5.131×10^4	40.58
	P2	1.187	408	1.87	5.491×10^4	38.90
	P3	1.207	441	2.02	1.037×10^5	46.40
	P4	1.290	472	1.44	1.649×10^5	41.90
	P5	1.572	505	1.63	2.148×10^5	42.05
	P6	1.638	536	1.78	8.907×10^4	47.66
	P7	1.664	575	2.10	7.721×10^4	58.59
	P8	1.748	628	2.5	5.245×10^4	72.73
TL (2Gy) [28]						
		E(eV)	*T_m(K)*	*b*	*n_0*	*w(K)*
Eu (0.2mol%)	P1	1.02	396	1.30	1.362×10^5	37.80
	P2	1.07	425	1.23	3.911×10^5	37.33
	P3	1.23	447	1.30	1.689×10^5	35.78
	P4	1.44	478	1.25	1.111×10^5	37.98
	P5	1.75	504	1.63	6.612×10^4	40.81
	P6	1.78	548	1.42	3.084×10^4	57.90
	P7	1.98	593	2.5	6.183×10^4	37.80
Dy (0.002mol%)	P1	0.93	430	1.10	2.05×10^5	41.70
	P2	1.09	456	1.28	6.29×10^4	48.06
	P3	1.33	487	1.44	4.8×10^4	46.06
	P4	1.40	522	1.55	2.38×10^4	54.16
	P5	1.68	570	2.5	2.65×10^4	56.62
Eu/Dy	P1	0.93	423	1.00	6.25×10^5	38.80
	P2	1.22	461	1.25	1.19×10^5	39.19
	P3	1.36	489	1.53	7.89×10^4	43.88
	P4	1.41	536	1.49	5.43×10^4	50.21
	P5	1.62	585	2.5	1.51×10^5	68.01

The initial concentration of trapped electrons within the defects centers was however noted to vary. Such variations in the population of electrons within the traps are indications of mobile defect states and charge conversion and/or transfer between defect states such that very shallow states and deep level states are emptying to moderate defect states. This has two main advantages on the efficiency, first; defect

states are becoming more stable since the temperature at maximum is increased and second; unwanted deep level states as well as surface defect states are minimized or even eliminated.

IV. CONCLUSION

Radiation induced defects and thermoluminescence characteristics in synthesis quartz samples were studied under 2Gy of beta dose and 2MeV $^4He^+$. The TL-response in the doped Eu^{3+}, Dy^{3+} and co-doped Eu/Dy synthesis quartz are very sensitive to type of ionizing radiation. The ionizing radiation also imparted an unstable TL signal which could potentially be beneficial for intrinsic dosimetry.

ACKNOWLEDGMENT

The authors would like to thank the University of Jordan for support.

REFERENCES

[1] Nupur Gupta, Hirdesh, Rajinder Kaur, Atul Khanna, Satbir Singh, Bipin Kumar Gupta. 2019. "Spatially resolved X-ray fluorescence, Raman and photoluminescence spectroscopy of Eu^{3+}/Er^{3+}doped tellurite glasses and anti-glasses", Jo. of Non-Cryst. Solids.513,24-35.

[2] G.C. Righini, M. Ferrari, 2005. Photoluminescence of rare-earth-doped glasses, Rivista de, lNuovoCimento 28 1–53.

[3] J. Rocha, L.D. Carlos, F.A.A.Paz, D.Ananias, 2011. Luminescent multifunctional lanthanides-based metal–organic frameworks, Chem. Soc. Rev.40, 926–940.

[4] S.Tanabe, 2002. Rare-earth-doped glasses for fiber amplifiers in broadband telecommunication. C R Chim**.** 5815–824.

[5] F.Agullo-Lopez, C. R. A.Catlow and P. D. Townsend, 1988. Point Defects in Materials (London: Academic Press).

[6] K.Awazu, 2004. Ablation and compaction of amorphous SiO_2irradiated with ArF excimer laser. J. Non-Cryst. Solids. 337(3)241-253.

[7] I.P. Jain, G.Agarwal, 2011. Ion beam induced surface and interface engineering. Surface Science Reports; 66: 77-172.

[8] M.C. Ridgway, R.Giulian, D.J.Sprouster, P.Kluth, L.L. Araujo, D.J. Llewellyn, et al. 2011. Role of thermodynamics in the shape transformation of embedded metal nanoparticles induced by swift heavy-ion irradiation. Phys. Rev. Lett. 106: 095505.

[9] W. J.Weber,D. M.Duffy,L.Thomé,&Y.Zhang,2015.The role of electronic energy loss in ion beam modification of materials.Curr. Opin. Solid State Mater. Sci.19, 1–11.

[10] Bu Wang,Yingtian Yu,Isabella Pignatelli,Gaurav Sant, *and*Mathieu Bauchy. 2015. Nature of radiation-induced defects in quartz. J. Chem. Phys.143, 024505;https://doi.org/10.1063/1.4926527.
M.Decreto, T. Shikama, and E.Hodgson, 2004. Performance of functional materials and components in a fusion reactor: the issue of radiation effects in ceramics and glass materials for diagnostics",J. Nucl. Mater. 329-333. (125).https://doi.org/10.1016/j.jnucmat.2004.04.012.

[11] International Conference on Ion Beam Modification of Materials, 30 Oct-04 Nov, 2016, Museum of New Zealand Te Papa Tongarewa,Wellington,New Zealand.

[12] IBMM 2018, 21st International Conference On Ion Beam Modification Of Materials, JUNE 24 – 29, 2018, SAN ANTONIO, TEXAS, USA.

[13] A. Kamarou, W. Wesch, E. Eendler, A. Undisz, and M.Rettenmayr, 2006. "Swift heavy ion irradiation of InP: Thermal spike modeling of track formation", Phys. Rev. B73, 184107.

[14] Y. Zhang, F. Gao, W. Jiang, D. E. McCready, and W. J. Weber, 2004. "Damage accumulation and defect relaxation in 4H−SiC", Phys. Rev. B70, 125203.

[15] S.M. F.Leclerc, A.Beaufort, J. F. Declémy, Barbot. 2008."Evolution of defects upon annealing in He-implanted 4H-SiC", Appl. Phys. Lett. 93(12): 122101.DOI:10.1063/1.2988262.

[16] D.Simeone, J. L.Bechade, D.D.Gosset, A.Chevarier, P. Daniel, H.Pilliaire, and G.Baldinozzi, 2000. "Investigation on the zirconia phase transition under irradiation",Jo. of Nucle. Mate. 281(2–3),171-181. doi.org/10.1016/S0022-3115(00)00183-5Get rights and content.

[17] Kasatkin I., F. Girgsdies, T. Ressler, R. A. Caruso, J. H. Schattka, J. Urban, and K. Weiss, 2004. "HRTEM observation of the monoclinic-to-tetragonal (m-t) phase transition in nanocrystalline ZrO_2", J. Mater. Sci.39.

[18] Y.Zhang, J.Lian, C. M.Wang, W.Jiang, R. C.Ewing, and W. J. Weber, 2005."Ion-induced damage accumulation and electron-beam-enhanced recrystallization in $SrTiO_3$",Phys.Rev.B 72.

[19] B.Boizot, S.Agnello, B.Reynard, R.Boscaino, and G.Petite, 2003. Raman spectroscopy study of β-irradiated silica glass", J. Non-Cryst. Solids. 325. 22-28.

[20] T.Souno, H. Nishikawa, M.Hattori, Y.Ohki, E.Watanabe, M.Oikawa, T.Kamiya, and K.Arakawa, "Characterization of ion-implanted silica glass by micro-photoluminescence and Raman spectroscopy", 2003. Nucl. Instrum. Methods Phys. ResB210,September 2003, Pages 277-280.

[21] L.Skuja, 1998. "Section 1. Defect studies in vitreous silica and related materials Optically active oxygen-deficiency-related centers in amorphous silicon dioxide", Journal of Non-Crystalline Solids.239 16-48.

[22] A. N.Truhkin, H.-J Fiting, Investigation of optical and radiation properties of oxygen deficient silica glasses,1999. J. Non-Cryst. Solids. 248, pp.49-64.

[23] M.Watanabe, T.Yoshida, T.Tanabe, S.Muto, A.Inoue, and S.Nagata, 2006. Observation of defect formation process in silica glasses under ion irradiation, 2006. Nucl. Instr. And Meth. In Phys. Res.B250174-177**.**

[24] S.Nagata, S.Yamamoto, K.Toh, B.Tsuchiya, N.Ohtsu, T.Shikama, and H.Naramoto, 2004. Luminescence inSiO_2induced by MeV energy proton irradiation,J. Nucl. Mater.329(1), 1507–1510.

[25] S.Nagata, S.Yamamoto, A.Inouye, K.Toh, B.Tsuchiya, B.Tsuchiya, and T.Shikama, 2007. Luminescence characteristics and defect formation in silica glasses under H and He ion irradiation", J. Nucl. Mater.3671009-1013.

[26] Y.Zhang, F.Gao, W.Jiang, D. E.McCready, and W. J.Weber, 2004. Damage accumulation and defect relaxation in4H−SiC", Phys. Rev. B 70125203.

[27] McKeever S W S, 1985. Thermoluminescence of Solids(London: Cambridge University Press).

[28] F.Agullo-Lopez, C. R. A.Catlow and P. D. Townsend 1988. Point Defects in Materials(London: Academic Press).

[29] S. W. S.McKeever, M.Moskovitch, and P.D.Townsend, 1995. Thermoluminescence Dosimetry and Materials, Properties and Uses. Nuclear Technology Publishing England.

[30] F.Khamis, and D. E. Arafah, 2017. Synthesis, Characterization and Thermoluminescence Properies of Rare Earth Ions Doped Silica Glass Prepared by Sol-Gel Technique. 2017. AJOPACV, 3(2): 1-12, No. 36403.

[31] A.Sbouh, D-E. Arafah, and Y.Al-Ramadin, 1989. "Radiation enhanced diffusion of Ag produced by Ar implantation intoAg-doped glass".J. Phys.: Condens. Matter 1. 5045-5050.

[32] D.-E.Arafah, and R.Ahmad-Bitar, 2000. Induced defects and structural changes resulting from the processing of CdTe and CdS thin film. Solar Energy Materials & Solar Cells 64. 45-54.

[33] S.Hufner, OpticalSpectra of Transparent Rare-Earth Compunds (Academicm New York, 1978).

[34] T.Yang, Y.Gao, X.Huang, Y. Zhang, M. Toulemonde, J. Xue, A. Yan, and Y. Wang, 2011. The transformation balance between two types of structural defects in silica glass in ion-irradiation processes. J. Non-Crystalline Solids357. 3245-3250.

[35] K. Kajihara, M. Hirano, L. Skuja, and H. Hoson, 2008. Intrinsic defect formation in amorphous$SiO_2$by electronic excitation: Bond dissociation versus Frenkel mechanisms",Phys. Rev. B;78, 094201.

[36] M. M. Ma, X. Chen, K. Yang, Y. Sun, Y. Jin, and Z. Zhu, 2010. Color center formation in silica glass induced by high energy Fe and Xe ions, Nucl. Instrum. Methods Phys. ResB; 268. 67-72.

[37] N. Yazici, 1998. Determination of temperature dependent frequency factor constant from glow curve. Tr. J. of Physics; 22. 415-419.

[38] T. Igarashi, K. Kusunoki, T. Ohno, Isobe and M. Senna, 2002. Nanoparticles surface engineering of ultra-dispersedpoly tetrafluoroethylene. Mater. Res. Bull.37. 533.